

References

- 1 J.-M. Triscone, M. G. Karkut, L. Antognazza, O. Brunner and Ø. Fischer, *Phys. Rev. Lett.*, **63** (1989) 1016.
- 2 J.-M. Triscone, Ø. Fischer, O. Brunner, L. Antognazza, A. D. Kent and M. G. Karkut, *Phys. Rev. Lett.*, **64** (1990) 804.
- 3 Q. Li, X. X. Xi, X. D. Wu, A. Inam, S. Vadlamannati, W. L. McLean, T. Venkatesan, R. Ramesh, D. M. Hwang, J. A. Martinez and L. Nazar, *Phys. Rev. Lett.*, **64** (1990) 3086.
- 4 D. H. Lowndes, D. P. Norton and J. D. Budai, *Phys. Rev. Lett.*, **65** (1990) 1160.
- 5 A. Gupta, R. Gross, E. Olsson, A. Segmüller, G. Koren and C. C. Tsuei, *Phys. Rev. Lett.*, **64** (1990) 3191.
- 6 T. Matsushima, Y. Ichikawa, H. Adachi, K. Setsune and K. Wasa, *Solid State Commun.*, **76** (1990) 1201.
- 7 M. Kanai, T. Kawai and S. Kawai, *Appl. Phys. Lett.*, **57** (1990) 198.
- 8 I. Bozovic, J. N. Eckstein, M. E. Klausmeier-Brown and G. Virshup, *J. Superconductivity*, in the press.
- 9 O. Brunner, L. Antognazza, J.-M. Triscone, L. Miéville and Ø. Fischer, *Phys. Rev. Lett.*, **67** (1991) 1354.
- 10 J.-M. Triscone, L. Antognazza, O. Brunner, L. Miéville, M. G. Karkut, O. Eibl, P. van der Linden, J. A. A. J. Perenboom and Ø. Fischer, *Physica C*, **185-189** (1991) 210.
- 11 D. Lew, Y. Suzuki, C. B. Eom, M. Lee, J.-M. Triscone, T. H. Geballe and M. R. Beasley, *Physica C*, **185-189** (1991) 2553.
- 12 C. B. Eom, A. F. Marshall, J.-M. Triscone, S. S. Laderman, B. Wilkens and T. H. Geballe, *Science*, **251** (1991) 780.
- 13 J. B. Barner, C. T. Rogers, A. Inam, R. Ramesh and S. Bersey, *Appl. Phys. Lett.*, **59** (1991) 742.
Y. Tarutani, T. Fukazawa, U. Kabasawa, A. Tsukamoto, M. Hiratani, M. Suga and K. Takagi, *Proc. 3rd FED Workshop, Kumamoto, May 1991*, in press.
- 14 C. B. Eom, J.-M. Triscone, Y. Suzuki and T. H. Geballe, *Physica C*, **185-189** (1991) 2065.
- 15 A. R. Sweedler, Ch. J. Raub and B. T. Matthias, *Phys. Lett.*, **15** (1965) 108.
- 16 C. B. Eom, J. Z. Sun, B. M. Lairson, S. K. Streiffer, A. F. Marshall, K. Yamamoto, S. M. Anlage, J. C. Bravman, T. H. Geballe, S. S. Laderman, R. C. Taber and R. D. Jacowitz, *Physica C*, **171** (1990) 354.
- 17 C. B. Eom, A. F. Marshall, S. S. Laderman, R. D. Jacowitz and T. H. Geballe, *Science*, **249** (1990) 1549.
- 18 N. G. Stoffel, P. A. Morris, W. A. Bonner and B. J. Wilkens, *Phys. Rev. B*, **37** (1988) 2297.
- 19 Y. Iye, T. Tamegai, T. Sakakibara, T. Goto, N. Miura, H. Takeya and H. Takai, *Physica C*, **153-155** (1988) 26.
- 20 U. Welp, W. K. Kwok, G. W. Crabtree, K. G. Vandervoort and J. Z. Liu, *Phys. Rev. Lett.*, **62** (1989) 1908.
- 21 O. Brunner, J.-M. Triscone, L. Antognazza, M. G. Karkut and Ø. Fischer, *Physica B*, **165-166** (1990) 469.
- 22 T. Terashima, K. Shimura, Y. Bando, Y. Matsuda, A. Fujiyama and S. Komiyama, *Phys. Rev. Lett.*, **67** (1991) 1362.
- 23 T. P. Orlando and K. A. Delin, *Foundations of Superconductivity*, Addison-Wesley, Reading, MA, 1991, p. 388.
- 24 T. T. M. Palstra, B. Batlogg, R. B. van Dover, L. F. Schneemeyer and J. V. Waszczak, *Phys. Rev. B*, **41** (1990) 6621.
- 25 T. T. M. Palstra, B. Batlogg, L. F. Schneemeyer and J. V. Waszczak, *Phys. Rev. B*, **43** (1991) 3756.

Structure and magnetic properties of the rare earth fluoride, Ho_2CF_2 [†]J. K. Cockcroft[†], R. I. Cowell, Max-Planck-Institut für Physik der Materie (FRG)

(Received July 1, 1991; accepted August 1, 1991)

Abstract

The preparation of a new rare earth fluoride, space group $P\bar{3}1$ at low temperature. On cooling it becomes an antiferromagnet with magnetic structure $P\bar{1}$ due to magnetoelastic coupling. Evidence from high resolution neutron diffraction measurements show the dimensionality of the structure is discussed.

1. Introduction

The chemistry of rare earth compounds has been a review of the chemistry of the rare earths). In rare earth compounds the metal atoms are condensed to structures. In all the rare earth compounds the metal atoms are condensed to structures. In all the rare earth compounds the metal atoms are condensed to structures.

So far, only one rare earth compound, Ho_2CF_2 , in addition to the reports on the preparation of holmium fluoride, Ho_2CF_2 .

*Dedicated to Professor R. I. Cowell on his 60th birthday.

[†]Also at Institut Laue-Langevin, Grenoble, France.

gely characterized by the presence of extended bilayers and the highly isotropic chemical bonding associated with them, implying interesting magnetic and electrical properties.

Experimental details

Sample preparation and characterization

The starting materials, holmium, HoF_3 and carbon, were prepared as follows. Sublimed holmium metal lumps (99.99%, Universal Matthey, Karlsruhe) were heated in a molybdenum crucible under hydrogen for 2 h at 900 to produce holmium hydride. This was ground and then dehydrogenated at 1100 K for 5 h under high vacuum to yield powdered holmium metal. F_3 was prepared from Ho_2O_3 (99.99%, Universal Matthey) and HF following the method described by Greis and Petzel [4]. Carbon, in the form of activated charcoal (high purity, Merck, Darmstadt), was degassed at 1450 K in high vacuum for 24 h and stored in a pure argon atmosphere.

Of the rare earth carbide fluorides, the holmium derivative was thought to be easy to prepare owing to the fact that HoF_3 exhibits one of the lowest melting points of all the rare earth trifluorides. Ho_2CF_2 was synthesized from the starting materials holmium, HoF_3 and carbon in the molar ratio 4:2:3 (total mass approximately 2.5 g) sealed under 1 bar of argon in a tantalum ampoule, which was then sealed under vacuum in a quartz glass tube and heated to 1450 K for 8 days, resulting in the formation of a single-phase polycrystalline dark brown Ho_2CF_2 powder. Ho_2CF_2 slowly decomposes in air and is readily dissolved by dilute mineral acids at ambient temperature.

X-ray investigations

Powdered samples of Ho_2CF_2 were characterized at room temperature using the modified Guinier technique [5] with silicon ($a = 5.43035 \text{ \AA}$) as an internal standard using $\text{Cu K}\alpha_1$ ($\lambda = 1.54056 \text{ \AA}$). The diffraction patterns, which index as trigonal, matched those of the isostructural gadolinium compound Gd_2CF_2 [3] with space group $P\bar{3}m1-D_{3d}^3$ (no. 164). The lattice constants, determined from coincidence measurements of 13 reflections in the range $4^\circ < \theta < 30^\circ$ ($\Delta\theta = \pm 0.005^\circ$) refined [6] to $a = 3.6567(2) \text{ \AA}$ and $c = 6.3171(5) \text{ \AA}$. The 20 largest d spacings (\AA) are (with relative intensities) 17(10), 3.167(60), 2.831(100), 2.236(70), 2.106(5), 1.828(60), 1.754(50), 1.683(10), 1.582(40), 1.579(5), 1.536(30), 1.416(20), 1.413(10), 1.381(10), 1.366(20), 1.263(5), 1.197(10), 1.195(10), 1.176(40) and 1.119(20).

Specific heat

The specific heat was measured in an adiabatic calorimeter designed for the examination of small samples [7]. Powder samples with typical masses about 500 mg were put in Duran glass ampoules and sealed under helium to ensure good thermal contact.

The magnetic contribution C_m to the heat capacity was obtained by subtracting a lattice contribution C_l which was estimated according to the

following procedure. A temperature was derived from the specific heat

$$C_p = 9R \left(\frac{T}{\Theta_D} \right)^3 \int_0^{\Theta_D/T} \frac{e^x x^4}{(e^x - 1)^2} dx$$

At high temperature a plot of C_p was extrapolated to low temperature to give the lattice part of the heat capacity, C_l . C_m was then obtained by numerically integrating C_m/T from $C_m = C_p - C_l$, following the method of

$$S_m(T) = \int_0^T \frac{C_m(T')}{T'} dT'$$

2.4. Magnetic susceptibility

The magnetic susceptibility of powder samples was determined with a Quantum Design SQUID magnetometer. The samples were contained in dried gelatin capsules and measured in separate runs and corrected for diamagnetic contributions.

2.5. Electrical conductivity

The resistance was determined using a two-point electrometer method. The samples were mounted on steel pistons and cooled with liquid nitrogen.

2.6. Neutron diffraction

For the neutron diffraction experiment, a single crystal of Ho_2CF_2 was sealed under helium gas in a vanadium can in diameter which was then submerged in a 6 mm diameter liquid helium bath. Diffraction patterns were recorded on a Laue-Langevin, Grenoble neutron diffractometer using a 400-wire $^3\text{He-Xe}$ gas multiwire detector. The temperature was scanned at 0 K (for 10 data were stored at approximately 0 K for technical reasons). In addition, quick scan patterns were recorded in the absence of further phase resolution patterns of Ho_2CF_2 in the 2θ range 6° – 156° in steps

3. Results and discussion

The structure of Ho_2CF_2 was determined from the $P\bar{3}m1$ by the Rietveld method

D1A data collected on the sample at 50 K. From the 2900 data points containing 48 contributing reflections, a total of 13 parameters (of which six are structural) were refined. The final parameters, which are uncorrected for the effects of absorption, are shown in Table 1, with the best fit to the data displayed in Fig. 1. The correction to the temperature factors due to the effect of absorption is estimated at about 0.2 \AA^2 .

Figure 2 shows a projection of the structure along [110]. The structure may be described in terms of Ho_6 octahedra filled with carbon atoms which are connected via their edges to form infinite $[\text{Ho}_2\text{C}]$ layers. The coordination of the remaining edges by fluorine atoms results in $[\text{Ho}_2\text{C}]$ layers sandwiched between fluorine layers and stacked along [001] according to the sequence $\cdots\text{Ab}\gamma\text{aB}\cdots$ ($\cdots\text{FHoCHoF}\cdots$). Such FHoCHoF layers are held together by van der Waals forces. Owing to the trigonal symmetry, only two short metal-metal distances are found: the shortest (3.41 \AA) is between the planes of the metal bilayers and the second, within the plane, is equal to the lattice constant a (3.65 \AA).

The structure type is well known from a great number of different compounds such as $\text{Gd}_2\text{Br}_2\text{C}$ [10], CaAl_2Si_2 [11], $\text{Ta}_2\text{S}_2\text{C}$ [12], $\text{Ce}_2\text{O}_2\text{S}$ [13] and Ln_2O_3 [14], which have structural subunits $[\text{CGd}_2]$, $[\text{CaSi}_2]$, $[\text{CTa}_2]$, $[\text{SCe}_2]$ and $[\text{OLn}_2]$ respectively based on the CdI_2 structure [15]. The remaining atoms fill the tetrahedral holes between the metal or silicon double layers.

Conductivity experiments show that Ho_2CF_2 is non-metallic as predicted by the simple ionic description $(\text{Ho}^{3+})_2\text{C}^{4-}(\text{F}^-)_2$. The resistance of the measured pellet is of the order of several megaohms at room temperature and increases by three orders of magnitude on cooling to liquid helium temperature. The result is similar to that observed for the layered metal-rich rare earth halides in which all voids in the metal atom bilayer are fully

TABLE 1

Final parameters, R factors and interionic distances for Ho_2CF_2 at 50 K. R factors are defined as in ref. 8 with $y_i(\text{obs})$ referring only to the Bragg intensity, *i.e.* $y_i(\text{obs}) = y_i(\text{total}) - y_i(\text{background})$. Weights are given by $1/\sigma_{y_i(\text{obs})}^2$. Scattering lengths $\text{Ho} = 8.37 \text{ fm}$, $\text{C} = 5.65 \text{ fm}$, $\text{F} = 6.65 \text{ fm}$ [22]. $\lambda = 1.911 \text{ \AA}$. Space group $P\bar{3}m1$. $a = 3.65373(1) \text{ \AA}$, $c = 6.3098(2) \text{ \AA}$. $V = 72.949(2) \text{ \AA}^3$, $\rho_{\text{calc}} = 8.646 \text{ g cm}^{-3}$

Atom	Site symmetry	X	Y	Z	B (\AA^2)	N
Ho	2d $3m$	$\frac{2}{3}$	$\frac{1}{3}$	0.7876(6)	-0.16(7)	2
C	1a $3m$	0	0	0	0.07(14)	1
F	2d $3m$	$\frac{2}{3}$	$\frac{1}{3}$	0.3882(6)	0.51(10)	2

U, V, W (deg^2): 0.172(5), -0.423(13), 0.365(7)

$R_{\text{wp}} = 6.3\%$, $R_{\text{exp}} = 3.6\%$, $R_1 = 3.8\%$

Interatomic distances (\AA)

Ho-Ho	3.411(4), 3.653(1)	Ho-C	2.499(2)	Ho-F	2.520(5), 2.383(3)
F-F	2.538(3)	F-C	3.233(3)		

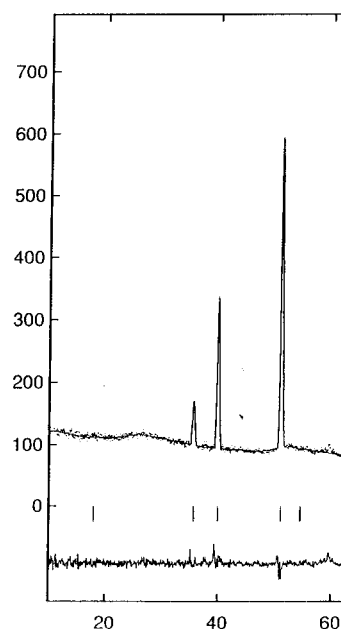


Fig. 1. Observed, calculated and with $\lambda = 1.911 \text{ \AA}$. Vertical tick marks estimated by graphical methods, decreases as the holmium form of the background are due to diffu

filled with hydrogen inters the rare earth halide dicar formulated as $(\text{RE}^{3+})_2(\text{C}^{4-} \text{ covalent interaction of the states.$

The specific heat (Fig 3.61(5) K and a long tail to up to 25 K. The specific heat to be of antiferromagnetic moments (Fig. 4). The latter ϵ below. The derivative $d(\chi T)$ at 3.7(1) K in agreement with susceptibility follows a Cu

$$\chi_{\text{mol}} = \frac{C}{T - \Theta}$$

with a paramagnetic Curie predominantly antiferromag

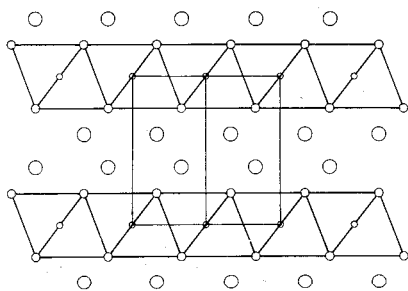


Fig. 2. Projection of the structure as seen down [110]. Holmium, carbon and fluorine are represented by medium, small and large circles respectively.

Fig. 3. (a) Specific heat C_p and estimated lattice heat capacity C_l (full curve) of Ho_2CF_2 . (b) Magnetic part S_m of the entropy according to eqn. (2). (All data are per one formula unit of $\text{HoC}_{0.5}\text{F}$.)

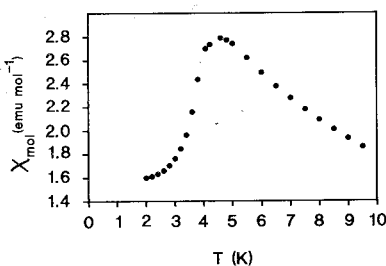


Fig. 4. Molar magnetic susceptibility χ_{mol} of Ho_2CF_2 at low temperatures.

C corresponds to an effective magnetic moment of $9.4 \mu_B$, which is slightly lower than the expected free-ion value of $10.6 \mu_B$.

From the diffraction patterns collected on D1B (Fig. 5) it is evident that between 1.5 K and room temperature Ho_2CF_2 exhibits only one phase transition at about 4 K, in agreement with the specific heat (Fig. 3) and magnetic susceptibility (Fig. 4) measurements. The extra peaks that appear at low temperature in Fig. 5 are attributed to antiferromagnetic ordering of the magnetic spins of the Ho^{3+} ions and may be indexed in terms of a doubling of the trigonal unit cell along a with consequent loss of threefold symmetry. Several magnetic space groups are possible and the correct structure was determined by trial and error to have the magnetic space group symmetry $P_a\bar{1}'$.

The complete magnetic structure was refined by the Rietveld method from the D1A data of Ho_2CF_2 at 1.5 K (Fig. 6) using the program MPROF

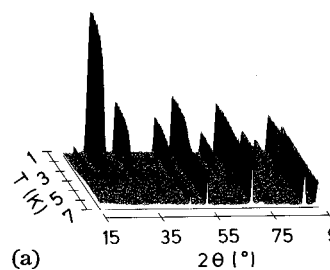
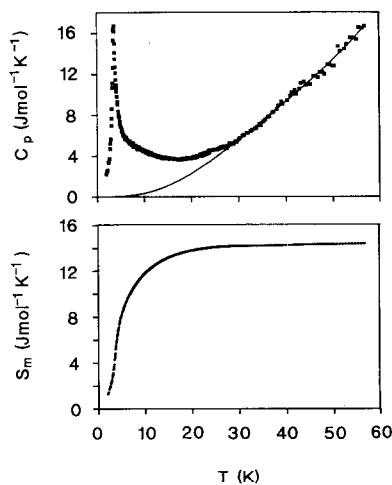


Fig. 5. (a) Diffraction patterns obtained on heating on D1B with artefact due to a bad wire of reflections $\frac{1}{2}00$ (upper) and $\frac{1}{2}01$

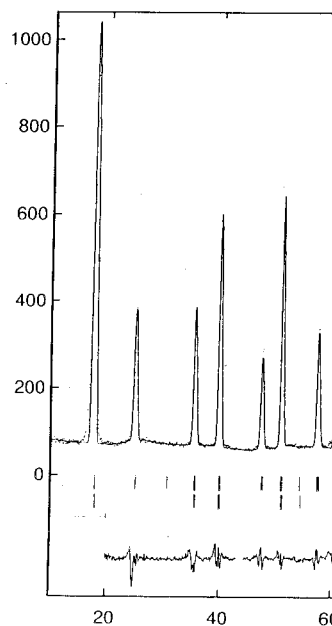


Fig. 6. Observed, calculated and with $\lambda = 1.911 \text{ \AA}$. Upper and lower and nuclear reflections respectively. Rietveld least-squares refinement background is considerably reduced.

[18] with the reflection c and $\gamma \approx 120^\circ$. The magnetic Brown [19]. During the refinement for the cell constants were refined converged to I

of the D1A data shows that the nuclear peaks are split at high angle and this is readily seen for the peak at 98.7° in Fig. 6 where the diffractometer has its best resolution. Removal of the symmetry conditions applied to the cell constants gave a significantly better fit to the data with $R_{wp} = 11.4\%$. However, it was apparent from the difference profile that the magnetic peaks were slightly broadened with respect to the nuclear peaks and a multiphase fit to the data was carried out with separate U , V and W parameters to describe the peak widths as a function of 2θ for the nuclear and magnetic peaks. The best fit to the data, shown in Fig. 6, with $R_{wp} = 9.0\%$, was achieved with 23 parameters (of which nine are structural) in which the x , y coordinates of Ho and F were fixed at 0.6667, 0.3333 as in the trigonal structure and with the intense magnetic peak at 17.9° excluded from the refinement owing to instrumental asymmetry effects. The final parameters and R factors are listed in Table 2.

The arrangement of the magnetic moments corresponds to an antiferromagnetic collinear structure with the propagation vector along [100]. In the ab plane the components of the magnetic moments lie 17° off the [010] direction and are tilted out of the ab plane by 24° as illustrated in Fig. 7. The total magnetic moment refined to $7.63(5) \mu_B$.

An interesting result of the high resolution D1A data analysis is the observation of lattice deformation due to magnetoelastic effects. The magnitude of this distortion is very small and is generally not observable in the low resolution diffraction patterns commonly used to determine magnetic structures on D1B. The difference between the a and b lattice constants is of the order of 0.02% and the angles deviate from those of the trigonal lattice by only 0.2%. The reduction in symmetry from $P\bar{3}m1$ to $P\bar{1}$ on transforming to the low temperature antiferromagnetic phase is consistent in terms of subgroup-supergrupp relationships with the observation of the colour space

TABLE 2

Final parameters and R factors for Ho_2CF_2 at 1.5 K. $\lambda = 1.911 \text{ \AA}$. Nuclear space group $Pa\bar{1}$, magnetic space group $P_3\bar{1}'$. $a = 3.6517(2) \text{ \AA}$, $b = 3.6510(2) \text{ \AA}$, $c = 6.3085(2) \text{ \AA}$, $\alpha = 90.121(5)^\circ$, $\beta = 89.808(3)^\circ$, $\lambda = 119.893(3)^\circ$. $V = 72.918(4) \text{ \AA}^3$, $\rho_{\text{calc}} = 8.642 \text{ g cm}^{-3}$

Atom	Site symmetry	X	Y	Z	$B (\text{\AA}^2)$	N
Ho	2i 1	0.6667	0.3333	0.7859(6)	-0.14(5)	2
C	1a $\bar{1}$	0	0	0	-0.01(10)	1
F	2i 1	0.6667	0.3333	0.3858(6)	0.36(9)	2

$M (\mu_B)$: 7.63(5)

$k_x, k_y, k_z (\mu_B)$: -2.34(13), 5.46(6), 3.19(9)

$U, V, W (\text{deg}^2)$ (nuclear): 0.17(1), -0.37(2), 0.33(1)

$U, V, W (\text{deg}^2)$ (magnetic): 0.38(2), -0.87(3), 0.65(1)

$R_{wp} = 9.0\%$, $R_{\text{exp}} = 6.4\%$, $R_1 = 4.4\%$, $R_1(\text{nuclear}) = 2.0\%$, $R_1(\text{magnetic}) = 7.5\%$

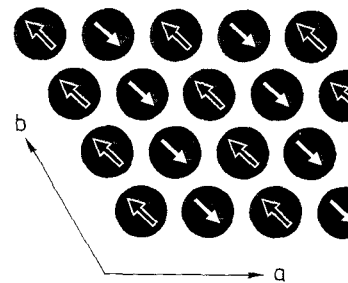


Fig. 7. View of the magnetic structure in the ab plane. Black and white arrows indicate magnetic moments.

group $Pa\bar{1}'$ for the magnetic structure. The magnetic moments are only available for 1.5 K. The onset of long-range antiferromagnetic order is uncommon for rare earth compounds.

At 1.5 K the difference between the nuclear and magnetic reflections is attributed to the lattice distortion. This is not so surprising as the onset of long-range antiferromagnetic order is uncommon for rare earth compounds. The difference between the a and b lattice constants is of the order of 0.02% and the angles deviate from those of the trigonal lattice by only 0.2%. The reduction in symmetry from $P\bar{3}m1$ to $P\bar{1}$ on transforming to the low temperature antiferromagnetic phase is consistent in terms of subgroup-supergrupp relationships with the observation of the colour space

The temperature dependence of the magnetic reflections obtained from the analysis of the data around 3.7(1) K in good agreement with the data from specific heat and susceptibility measurements. The onset of T_N observed for Ho_2CF_2 is unusual for layered metal-rich rare earth compounds, e.g. REX_2 ($\text{RE} = \text{Gd, Tb, Dy}$) at temperatures for metallic compounds. The magnetic moments are about one order of magnitude smaller than the f -electrons excludes RKKY interactions. The short-range dipolar coupling via the Ho^{3+} magnetic moments is not negligible, Ho_2CF_2 is no exception.

Owing to crystal field splitting the magnetic moment is lower than the

for the 5I_8 ground term (Landé factor $g_J = \frac{5}{4}$) of Ho^{3+} with $4f^{10}$ electronic configuration. In Ho_2CF_2 the degeneracy of the ground term is lifted by a crystal electric field of C_{3v} symmetry, in principle allowing that Ho_2CF_2 could *a priori* be diamagnetic at low temperatures, with a singlet as the crystal field ground state, which obviously is not the case for Ho_2CF_2 . The magnetic entropy is found to be $14.4 \text{ J mol}^{-1} \text{ K}^{-1}$ or $R \times 1.73$, being close to $R \ln 6$ (Fig. 3), and indicates the ordering of a six-level system. Such a large degeneracy for the crystal field ground state, on the other hand, seems unlikely in view of the low site symmetry. We suggest that a substantial part of the entropy also originates from the structural phase transition.

Assuming as a first approximation that the magnetic ordering takes place in a crystal field doublet as, for example, was observed for $\text{Ho}(\text{OH})_3$ [21], ground state eigenfunctions composed primarily of $J_z = \pm 6$ states could account for the experimentally detected magnetic moment of $7.63 \mu_B$. Inelastic neutron-scattering experiments should be carried out to establish the full crystal field level scheme of Ho^{3+} in Ho_2CF_2 in order to enable a detailed comparison with the results reported here.

Acknowledgments

We thank E. Brücher, H. Diem, R. Eger and W. Röthenbach for experimental help and E. Gmelin for very valuable discussions. N.P.R. gratefully acknowledges full financial support by the DAAD (German Academic Exchange Service).

References

- A. Simon, *J. Solid State Chem.*, **57** (1986) 2;
 H. J. Mattausch, C. Schwarz and A. Simon, *Z. Kristallogr.*, **178** (1987) 156;
 C. Bauhofer, H. J. Mattausch, G. J. Miller, W. Bauhofer and A. Simon, *J. Less-Common Met.*, **167** (1990) 65.
 A. Simon, H. J. Mattausch, G. J. Miller, W. Bauhofer and R. K. Kremer, in K. A. Gschneidner Jr. and L. Eyring (eds.), *Handbook on the Physics and Chemistry of Rare Earths*, Vol. 15, North-Holland, Amsterdam, 1991, p. 191.
 H. J. Mattausch, R. Eger and A. Simon, *Z. anorg. allg. Chem.*, **597** (1991) 145.
 O. Greis and T. Petzel, *Z. anorg. allg. Chem.*, **403** (1974) 1.
 A. Simon, *J. Appl. Crystallogr.*, **3** (1970) 1.
 K. F. Tebbe, Program AGL, *Ph.D. Thesis*, Universität Münster, 1970.
 E. Gmelin and K. Ripka, *Cryogenics*, **21** (1981) 177.
 H. M. Rietveld, *J. Appl. Crystallogr.*, **2** (1969) 65.
 J. K. Cockcroft, Program PROFIL V4.05: a Rietveld program for the refinement of crystal structures from single and multiphase powder neutron and synchrotron radiation data, Institut Laue-Langevin, Grenoble, 1991.
 U. Schwanz-Schüller and A. Simon, *Z. Naturf. B*, **40** (1985) 710.
 E. I. Gladyshevskii, P. I. Krypyakevich and O. I. Bodak, *Ukr. Fiz. Zh.*, **12** (1967) 454.
 O. Beckmann, H. Boller and H. Nowotny, *Monatsh. Chem.*, **101** (1970) 945.
 W. H. Zachariasen, *Acta Crystallogr.*, **2** (1949) 60.
 P. Adelbert and J. P. Traverse, *Mater. Res. Bull.*, **14** (1979) 303.

- 15 Z. G. Pinsker, *Zh. Fiz. Khim.*,
 16 H. J. Mattausch, R. Eger, R. K. 1
 17 M. E. Fisher, *Proc. R. Soc. (L*
 18 M. W. Thomas and P. J. Bend
 19 P. J. Brown, personal commur
 20 F. Lèvy, *Phys. Kondens. Mate*
 M. E. Mullen, B. Lüthi, P. S. .
Rev. B, **10** (1974) 186.
 21 C. A. Catanese and H. E. Meis
 22 L. Koester and H. Rauch, *Reco*
2517/RB, 1983 (International .